Flexibility of the Neck Domain Enhances Kinesin-1 Motility under Load

Johann Jaud,* Friederike Bathe,† Manfred Schliwa,† Matthias Rief,* and Günther Woehlke†
*Physics Department E22, Technical University Munich, Garching, Germany; and †Institute for Cell Biology, University of Munich, Munich, Germany

ABSTRACT Kinesin-1 is a dimeric motor protein that moves stepwise along microtubules. A two-stranded α-helical coiled-coil formed by the neck domain links the two heads of the molecule, and forces the motor heads to alternate. By exchanging the particularly soft neck region of the conventional kinesin from the fungus *Neurospora crassa* with an artificial, highly stable coiled-coil we investigated how this domain affects motor kinetics and motility. Under unloaded standard conditions, both motor constructs developed the same gliding velocity. However, in a force-feedback laser trap the mutant showed increasing motility defects with increasing loads, and did not reach wild-type velocities and run lengths. The stall force dropped significantly from 4.1 to 3.0 pN. These results indicate the compliance of kinesin's neck is important to sustain motility under load, and reveal a so far unknown constrain on the imperfect coiled-coil heptad pattern of Kinesin-1. We conclude that coiled-coil structures, a motif encountered in various types of molecular motors, are not merely a clamp for linking two heavy chains to a functional unit but may have specifically evolved to allow motor progression in a viscous, inhomogeneous environment or when several motors attached to a transported vesicle are required to cooperate efficiently.

INTRODUCTION

Kinesin-1 motors move along microtubules by a mechanism that involves two identical motor heads that are able to hydrolyze ATP in a microtubule-dependent fashion. The catalytic cycles of the heads pass through phases of weak and strong microtubule affinity, and are interlaced in a manner that guarantees that at each given time point at least one of the motor heads remains filament-bound. This alternating site mechanism generates a so-called hand-over-hand type of stepwise motility (1,2). For motility according to this mechanism it is essential for the motor to use two motor heads, and to couple the actions of these heads. Kinesin-1's α-helical coiled-coil neck domain links the heads mechanically, and mutations that disrupt the integrity of this coiled-coil are known to lose their ability to move by the hand-over-hand mechanism (3,4). Thus, the coiled-coil neck structure is essential for motor function. However, despite its importance, the primary amino acid sequences of fungal and animal Kinesin-1 neck domains strongly deviate from the optimal heptad pattern, and cause a rather weak α-helical coiled-coil structure (3,5–7). Curiously, fungal and animal neck sequences differ strongly among each other. These observations have caused ongoing, controversial discussion (8–10).

To investigate the influence of the specific sequence and the role of the imperfect coiled-coil for the mechanism of conventional kinesins, we exchanged the entire neck domain of the fungal Kinesin-1 from *Neurospora crassa* (NcKin) with a perfect coiled-coil heptad repeat sequence of the same length and phase (EIEALKA (11,12)), leading to the mutant NcKin-SN (''stable neck''; Fig. 1). Unfolding of this coiled-coil is very unlikely because a synthetic peptide of comparable length showed a melting temperature of ~140°C (12). The SN replacement left only seven NcKin neck residues unchanged (*red* in Fig. 1).

As a wild-type construct, we used a truncated NcKin motor ending at the C-terminal end of the hinge (residue 436), which was shown to have similar properties as the full length protein, was well expressed in *Escherichia coli* and stable in vitro (3). To be able to test the motility of the constructs in microscopic assays, both under multiple and single motor conditions, we added a part of the human kinesin stalk domain C-terminal to the hinge ($NcKin_{hTail}$, (3)). The stalk portion causes unspecific adsorption to glass coverslips as well as to carboxylated latex beads without influencing catalytic or motility properties of the constructs.

MATERIALS AND METHODS

Protein expression and purification

NcKin-WT (wild-type) and mutant proteins were expressed in *E. coli* and purified based on their affinity to microtubules (13–15). Briefly, *E. coli* cells were lysed, centrifuged, and incubated with paclitaxel-stabilized microtubules in the presence of AMP-PNP and apyrase in 100 mM Pipes·KOH, 2 mM $MgCl_2$, 1 mM EGTA, pH 6.8. Kinesins bound to microtubules were sedimented and released by 10 mM of ATP in the above buffer, supplemented with 200 mM KCl. Microtubules were finally removed by centrifugation, the kinesin-containing supernatant was stored with 10% (w/v) glycerole at −70°C.

The optical trapping apparatus

All experiments were performed in a custom-built optical trap in combination with a total internal reflection (TIRF) microscope for fluorescence microscopy (16). The optical trap is similar to the device described by Finer

Submitted February 1, 2006, and accepted for publication May 12, 2006.

Johann Jaud and Friederike Bathe contributed equally to this work.

Address reprint requests to Günther Woehlke, Tel.: 49-89-2180-75889; Fax: 49-89-2180-75882; E-mail: guenther.woehlke@lrz.uni-muenchen.de.

0006-3495/06/08/1407/06 $2.00

doi: 10.1529/biophysj.105.076265

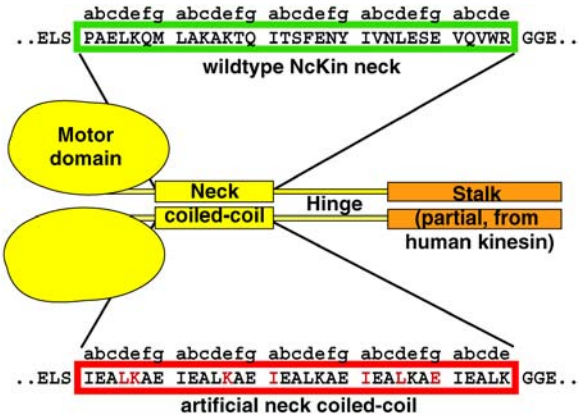

FIGURE 1 Design of a Kinesin-1 chimera with a stiff neck. To study the function of the Kinesin-1's neck coiled-coil, a NcKin Kinesin-1 reference construct was used that comprised the NcKin motor, neck, and hinge domains up to amino acid position 436. Part of the human stalk domain (human kinesin residues 432–546 (28)) was added C-terminal to the construct to allow unspecific attachment to glass slides or latex beads. The NcKin-SN mutant contained an artificial coiled-coil sequence of nearly five ''EIEALKA'' sequence repeats in place of the natural NcKin neck (*red box*; residues that are identical to the NcKin sequence are red). The length and phase of the heptad repeat pattern was identical to the wild-type.

et al. (17). The trapping laser was an 8 W Nd:YAG (Coherent Deutschland GmbH, Dieburg, Germany) focused through a high numerical aperture objective (NA = 1.45, Olympus Deutschland GmbH, Hamburg, Germany). The position of trapped beads was measured by bright field imaging onto a quadrant photo diode (SPOT4D, UDT Sensors, Hawthorne, CA). The sample was mounted on a piezo table (P-517.3CL, Physik Instrumente GmbH, Karlsruhe, Germany) controlled by a feedback loop over a digital signal processor board (M6x, Innovative Integrations, Simi Valley, CA). This feedback enables the observation of full processive runs of single molecular motors up to several micrometers in length without stalls. As the position of the trapped bead remains constant while a molecular motor is held under a constant force a correction of the position signal for the nonlinear behavior of the detector was not necessary. Data for the determination of run length, velocity, and stall force were acquired by an analog to digital converter board (MIO-16XE-50, National Instruments, Munich, Germany) with a sampling rate of 1 kHz per channel. For high-resolution traces as shown in Fig. 4, data were acquired by a high-performance analog to digital converter board (NI-PCI-6259, National Instruments) with a sampling frequency of 40 kHz per channel.

The trap stiffness was calibrated for each trapped bead separately from the amplitude of the thermal diffusion and for some beads cross-checked by fitting a Lorentzian to the power spectrum of the thermal diffusion (18). Both methods gave consistent results with typical trap stiffness values of 0.04–0.08 pN/nm.

Cy-5 labeled microtubules were visualized by total internal reflection microscopy using a HeNe laser (632 nm, Coherent Deutschland GmbH, Germany) and a high performance CCD camera (Pentamax Gen IV, Roper Scientific GmbH, Ottobrunn, Germany).

Microtubule gliding assays

All solutions used in the gliding assays were based on BRB80 buffer (80 mM PIPES-KOH, 2 mM $MgCl_2$, 1mM EGTA, pH 6.9). Flow cells with a volume of 10–15 μl were made by gluing a standard microscope cover slide on a microscope slide using silicone grease. After 3 min of incubation with 0.07 mg/ml BSA in BRB80 to preblock the surface 15 μl of the NcKin motor diluted to the desired concentration was washed into the cell. The motor was allowed to adsorb to the surface for 3 min at room temperature before nonadsorbed motor molecules were washed out with 100 μl BRB80 containing 1 mg/ml BSA. After 2 min at room temperature, 50 μl motility buffer consisting of BRB80 with 100 mM additional KCl, 0.5 mg/ml casein, 2 mM ATP and a variable concentration of microtubules were flowed through the fluid chamber before it was sealed by two additional stripes of silicon grease. All motility assays were performed at 23–24°C.

Optical trapping assays

Flow cells were prepared as described above and incubated for at least 15 min with a solution containing 0.1 mg/ml of a polyclonal tubulin antibody from sheep (ab1289, Acris Antibodies GmbH, Hiddenhausen, Germany). Excess, nonadhering antibodies were washed out with 100 μl 1 mg/ml BSA in BRB80 to block the surface followed by 15 μl diluted microtubule. After 3 min of incubation, excess microtubules were washed out by 100 μl BRB80 with 1 mg/ml BSA. For the preparation of the beads 5 μl of carboxylated polystyrene beads (532 nm, Polysciences, Warrington, PA) were rapidly mixed with equal amounts of 5 mg/ml Casein in BRB80 and diluted kinesin. The solution was stored on ice for at least 5 min, diluted 1:2000 in motility buffer containing 100 mM additional KCl, 0.5 mg/ml casein and 2 mM ATP and filled into the fluid chamber containing the immobilized microtubules. Beads were trapped and brought into contact with the surface bound microtubules.

To ensure data were acquired from single motor molecules we excluded all events from our analysis where more than 1/3 of the tested beads in a flow cell displayed movement when brought into contact with a microtubule (19).

Data analysis

TIRF motility assays were analyzed using ImageJ 1.32j (Wayne Rasband, National Institutes of Health), all other experiments were analyzed with IGOR Pro 4.01 (WaveMetrics, Portland, OR). Run lengths were tabulated manually by analyzing intervals that started when the desired force was reached, and ended by dissociation of the bead from the microtubule (>16 nm fall-back; typically 110–800 events).

Velocities were calculated from 0.1-s phases of continuous movement. Stall forces (Fig. 4) were measured under saturating ATP levels without force-feedback. Events were considered a stall and included in the statistical analysis if the motor could hold a constant force for at least 50 ms before releasing from the microtubule. The stall force was measured by averaging over a 50-ms interval of the stall plateau and subtracting the average of a 50-ms interval of the base line.

RESULTS

Biochemical characterization of the NcKin-SN mutant

To exclude artifacts due to improper dimerization the mutant motor with the artificial neck coiled-coil was studied in gel filtration and sucrose density centrifugation assays (3,14). As the human kinesin stalk forms a coiled-coil and thus leads to a dimeric molecule regardless of the structural state of the neck domain (3), constructs lacking the human stalk portion were used in these assays, ending with NcKin residue 436. As the wild-type control, the mutant clearly appeared as a dimer (83.4 and 72.6 kD versus the predicted molecular mass of 47.9 kD, Table 1), in agreement with the single molecule behavior described below. Noteworthy, constructs lacking the human tail portion did not adhere to latex beads, indicating that the motor attaches via the tail portion, and that all NcKin domains are free.

TABLE 1 Biochemical characterization of NcKin constructs

	Gliding velocity* [μm/s]		Molecular masses [kD]		
Construct	Multiple	Single	Derived	Predicted	Oligomerization state
NcKin-WT	1.49 ± 0.03	1.48 ± 0.03	83.4	47.9	Dimer
NcKin-SN	1.29 ± 0.02	1.49 ± 0.05	72.5	47.9	Dimer

*NcKin436 with human kinesin tail portion (HsKHC 432-546; (3)).

Microtubule gliding assays

To determine the velocity of microtubule translocation at different surface densities of kinesin, mutant and wild-type motors were assayed in a standard microtubule gliding assay (Table 1).

As in previous studies, the wild-type NcKin displayed fast motility under both multiple and single motor conditions ((1.49 ± 0.03) and (1.48 ± 0.03) μm/s), ~3 times faster than the corresponding human kinesin construct (11,20). The gliding velocity of the NcKin-SN construct in multiple motor assays was reduced (1.29 ± 0.02) μm/s compared to the wild-type. Under single molecule conditions NcKin-SN molecules supported smooth unidirectional transport of microtubules over a single anchoring point and pivoting of the microtubule around this point. The average gliding velocity of NcKin-SN under these conditions (1.49 ± 0.05) μm/s was indistinguishable from wild-type NcKin. This is in agreement with a previous study, where the replacement of the human kinesin neck coiled-coil by 4 heptads of the EIEALKA sequence also resulted in a decreased multiple motor velocity, but similar single motor motility (11).

Run lengths under different loads

To test whether NcKin-SN displays differences to wild-type under load, the run lengths of NcKin-WT and NcKin-SN mutant were measured under different backward forces in force-feedback mode (Fig. 2). Run length distributions of both molecules and under all measured forces followed a single exponential behavior (data not shown). NcKin-WT displayed a typical average run length of (480 ± 40) nm at 1.0 pN load, which decreased significantly under higher loads to (364 ± 10) nm at 2.0 pN and (192 ± 12) nm at 3.0 pN. The measured run lengths at all forces were shorter than previously published values measured in single molecule TIRF assays (20). Two points might explain this apparent discrepancy: i), our feedback system limits the observable run lengths to 3.2 μm and 5 s, and at low loads longer events were frequent; and ii), our feedback system directs the diffusion of a detached motor instantly away from the microtubule, thus preventing a possible rebinding in the vicinity.

Compared to wild-type NcKin the average run lengths of the stable-neck construct were significantly reduced under all forces tested. At 1.0 pN load NcKin-SN displayed an average run length of (297 ± 26) nm, which decreased further to (146 ± 10) nm at 2.0 pN, and (57 ± 12) nm at the highest measured load of 2.7 pN.

Single molecule velocities under different loads

The average velocities of single NcKin molecules under saturating ATP conditions were calculated from 1/10 s intervals of continued runs. Fig. 3 summarizes the results obtained for NcKin-WT and NcKin-SN under different loads.

For the lowest measured load of 0.7 pN NcKin-WT and NcKin-SN constructs both displayed high velocities of (2.04 ± 0.03) μm/s and (2.06 ± 0.02) μm/s, respectively, indicating the insertion of the EIEALKA sequence does not affect motility as long as the forces acting on the motor are low. Under an increased load the wild-type velocity was reduced by ~16% to (1.55 ± 0.02) μm/s at 2.0 pN, whereas the respective velocity for NcKin-SN dropped by ~52% to (0.99 ± 0.02) μm/s. At loads higher than 2.5 pN hardly any runs of NcKin-SN could be recorded that satisfied the criterion of 0.1 s of continuous movement for valid analysis.

Stall forces of single kinesin molecules

To determine the stall forces of NcKin-WT and -SN, the motility was observed in a microscopic bead assay in a static optical trap. Fig. 4, *A* and *B*, shows example traces of single NcKin-WT and NcKin-SN molecule runs in the optical trap at full bandwidth (40 kHz sampling frequency, *colored*) and

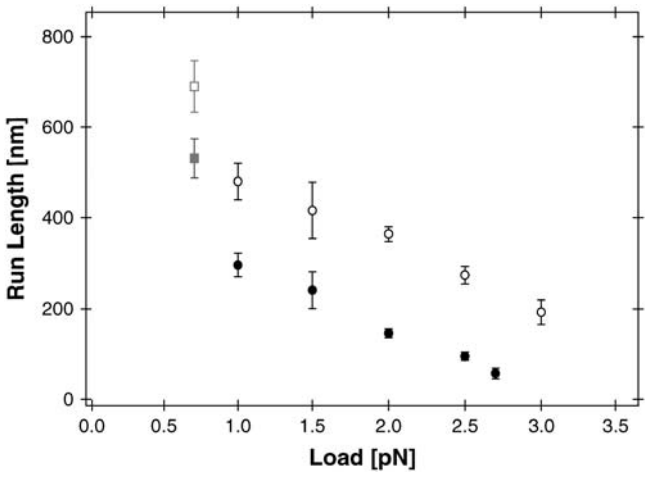

FIGURE 2 NcKin run lengths under load. Average run lengths *l* (mean ± SE) of NcKin-wild-type (*open circles*, $N = 50 - 477$) and NcKin-SN (*solid circles*, $N = 40 - 258$) versus applied load. All measurements were performed under constant force conditions. The data points at 0.7 pN (*gray squares*) are likely to present an underestimate due to the limited range of the feedback system. Both molecules display a significantly increasing processivity at loads smaller than 1.0 pN.

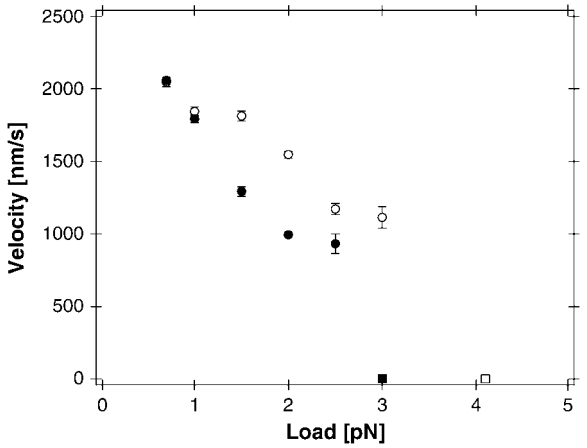

FIGURE 3 NcKin velocities under load. Average velocities v (mean ± SE) of NcKin reference (*open circles*, $N = 103 - 758$) and NcKin-SN (*solid circles*, $N = 73 - 512$) are plotted against applied load. The average velocities of both molecules drop with increasing external forces. Although both molecules display identical average velocities at the lowest tested loads of 0.7 and 1.0 pN, there are apparent differences at higher loads. The rectangles mark the molecules' stall forces where the average velocity is reduced to zero (Fig. 4).

filtered (1 kHz box filter, *black*) under saturating ATP concentrations. Near stall the filtered traces of both the mutant and the wild-type exhibit 8-nm steps. The unfiltered traces exhibit considerable noise reduction near stall. The position signal of the unbound bead showed a standard deviation of ~8 nm at a trap stiffness of 0.05 pN/nm, which was reduced to ~4 nm in bound beads at stall (~4 pN force), indicating that our experiments are not compromised by series compliance. Furthermore, individual 8-nm steps of wild-type NcKin were clearly discernable under limiting ATP concentrations (Supplemental Fig. S1).

Under saturating ATP concentrations stall forces of NcKin-WT molecules ranged from 2 to 7 pN with an average stall force of (4.1 ± 0.1) pN (Fig. 4 *C*, *green histogram*). The NcKin-SN construct displayed significantly reduced stall forces between 1 and 5 pN with an average of (3.0 ± 0.1) pN, 27% lower than the wild-type containing the natural neck domain (Fig. 4 *C*, *red histogram*). Moreover, a closer look at the traces revealed a qualitative difference between the two molecules: whereas NcKin-WT displayed long stall phases up to 1 s resulting in clear and easy to recognize plateaus, NcKin-SN molecules rarely showed stall phases longer than 0.1 s, and frequently detached before reaching a clear plateau. We also sometimes found limping of beads decorated with wild-type (21), but not consistently.

DISCUSSION

Mechanical flexibility in the neck domain is required for kinesin motility under load

Our findings indicate that a stiff Kinesin-1 neck coiled-coil impedes force generation. First, the average velocity is reduced under load and second, the run length of the stable

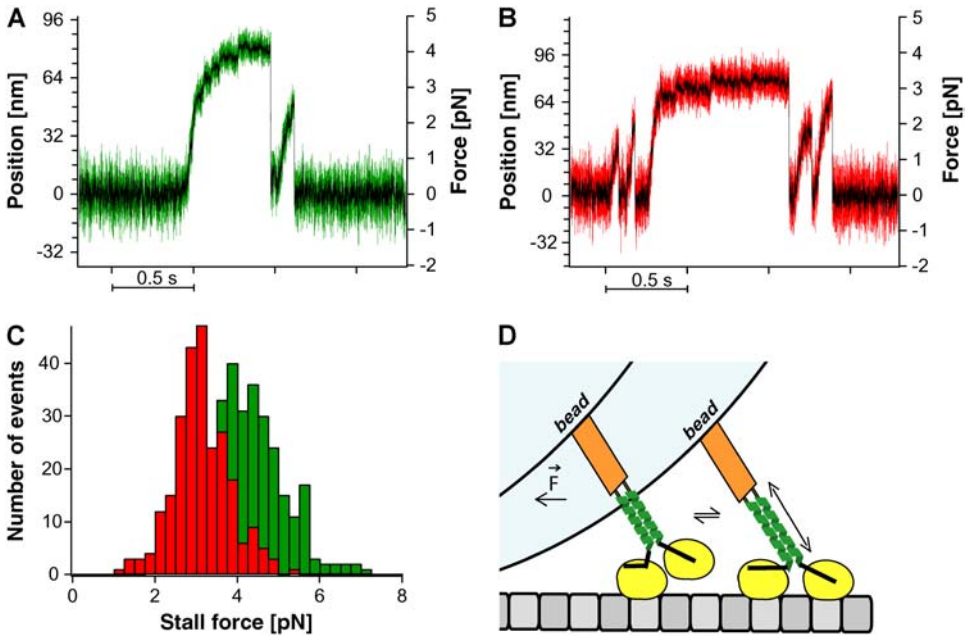

FIGURE 4 NcKin stall force measurements. Example traces of single-molecule runs of (*A*) NcKin wild-type (*green*) and (*B*) NcKin-SN mutant (*red*) in a static laser trap are shown. Data for both traces were acquired with a sampling rate of 40 kHz, the black trace is the 1-ms boxcar filtered signal. Although the wild-type molecule reaches forces above 4 pN, the stable neck mutant typically releases from the microtubule at forces ~3 pN. (*C*) Stall force distributions of the NcKin wild-type (*green*) and the NcKin-SN mutant (*red*). The average stall forces are 4.1 ± 0.1 pN ($n = 305$) for NcKin-WT and 3.0 ± 0.1 pN ($N = 251$) for NcKin-SN. (*D*) Model for the role of neck stiffness for kinesin stepping under load. We draw kinesin in an intermediate state where the neck-linker of the rear head is docked and the forward head searches its binding site. In this conformation, extension of the neck facilitates attachment. An extension of the natural, softer neck coiled-coil requires less energy than that of the artificial, stable neck and leads to optimized motility under load.

neck mutant is severely affected by external forces. Interestingly, these effects do not occur under unloaded conditions. What is the most likely reason for this behavior?

It has been proposed that the N-terminal neck segment may unfold transiently during the reaction cycle, supported by the fact that the two motor domains in the crystal structure of a dimeric kinesin cannot bridge the distance between neighboring microtubule binding sites and by the presence of unfavorable residues in the first half of the neck coiled-coil (22). At low load such neck unwinding is clearly not necessary because synthetic stiff or cross-linked neck coiled-coils still lead to motile kinesins (3,11,14,23). In agreement, this and previous studies of mutants of NcKin with a stiff or cross-linked neck show that they are as fast or nearly as fast as the wild-type. This indicates that under low load conditions the strong connection between the two motor domains mediated by the stable neck insert still allows for sufficient coordination of the two motor heads even for fast kinesins (3).

Our single molecule data suggest that the mechanical stability of the neck domain influences the motile properties of conventional kinesin. First, we find a strongly increased force sensitivity of the kinesin motor upon replacing the natural neck domain with an artificial, stable coiled-coil sequence. Although at low loads the difference between wild-type and mutant is either relatively minor (run length) or negligible (velocity), it is getting more pronounced with increasing force. Thus, at 2.0 pN the run length decreases to 60% compared to the wild-type. Second, the distorted motor functionality of the SN mutant under load is also reflected in the reduced average stall force of the molecule (3.0 compared to 4.1 pN). Since the insertion of the artificial neck domain leaves low load behavior of the motor almost unaffected but does change force production we suggest that the observed effects are not caused by the lack of specific fungal sequences, but by a decreased flexibility of the artificial neck domain. In line with this hypothesis both human and *Neurospora* kinesins are processive despite their considerably different neck sequences and coiled-coil properties.

Recent models of kinesin processivity propose rapid fluctuations of the free head along the microtubule lattice before it docks to the next binding site (24). According to our interpretation, the diffusional search of the unbound head is facilitated by the high compliance of the neck coiled-coil, which allows for forward progression of the newly leading motor head even when the molecule dwells in a loaded state (Fig. 4 *D*). As soon as the molecule experiences a substantial load, all flexible elements between the bead and the surface-anchored microtubule are stretched to a certain degree. After the kinesin neck linker has docked to the rear head upon the binding of ATP, the leading head faces in the forward direction (Fig. 4 *D*, *left*). Driven by Brownian motion it undergoes a diffusive search for the next microtubule binding site. In a loaded state the head has to ''borrow'' a part of the necessary coverage to reach this binding site from a flexible element in the molecule, presumably the kinesin neck coiled-coil. Energetically, this will be more costly and consequently more unfavorable for a stiffer coiled-coil.

Our model proposes the axial elasticity, not slippage between the two strands of the coiled-coil, as the source of elasticity that ensures smooth motor progression under external load. This view is supported by findings of Tomishige and Vale, who examined the load-dependent motility of a construct with an introduced cross-link at the beginning of the neck coiled-coil of human kinesin (23). They found no difference in velocities of the cross-linked and non-cross-linked motor under load, and only a subtle effect on the run length. Since introducing a cross-link into the otherwise unchanged neck would likely not affect neck stiffness, one would not expect a huge effect from such a construct. The stable coiled-coil neck used in our study, however, will have a significantly higher axial stiffness than the wild-type neck, leading to the observed increase in force sensitivity. We cannot exclude that torsional stiffness also contributes to the flexibility but since rotation and stretching may be coupled in a helical structure this does not add a new quality and a distinction cannot be made at this point. In a study examining the alternation of dwell times during stepping of kinesin molecules in an optical trap, two possible mechanisms have been proposed that induce limping (21). One involves slippage of the neck coiled-coil register, the other an asymmetry of the torsional compliance of the coiled-coil. Both mechanisms would be affected by the introduction of a stable coiled-coil element, and a change of the limping behavior would be expected. Our stable coil construct may hence be an interesting system for future investigation of limping behavior near stall. Although we do observe limping in some traces (see supplemental Fig. S1, Supplementary Material) we did not see it consistently. This may have to do with the total length of the neck used (21). The direct measurement of neck stiffness by force spectroscopy (25) might further clarify the role of axial versus torsional stiffness.

An interesting corollary of our study concerns the influence of neck charge on NcKin processivity under low load. Earlier studies indicated that neck net charge fine-tunes processivity of conventional kinesins through interactions of the positively charged neck coiled-coil and the negatively charged C-terminus of the microtubule (26,27). In contrast, NcKin wild-type shows long run lengths even though it carries no net charge. Also, the SN mutant although carrying four net negative charges only shows a slightly reduced run length. We suggest mechanical compliance of the neck coiled-coil as an additional source for high processivity.

CONCLUSIONS

In conclusion, our results suggest that the specific and conserved sequences of conventional kinesin neck domains have evolved to meet different, almost conflicting demands on motor functionality: a tight connection to provide

coordinated action of the two motor heads, and a flexible tether that enables optimal motor progression under extreme load conditions. Compliance might also be required when several motors are attached to one transported vesicle and have to cooperate efficiently. The reduced flexibility of the mutant neck obviously leads to significantly increased force sensitivity, and a motor with a stiffer neck would thus be less adapted to work as a molecular transporter in a crowded cellular environment where forces in the pN regime are likely to occur. Therefore, the coiled-coil in the kinesin neck is not only a clamp that links two heavy chains to allow communication between the two motor heads. It also provides the necessary compliance for the individual kinesin heads such that they can still reach out and find their forward microtubule binding site under load.

SUPPLEMENTARY MATERIAL

An online supplement to this article can be found by visiting BJ Onine at http://www.biophysj.org.

We thank Katrin Hahlen, Sarah Adio, and Melanie Reisinger for fruitful discussions, and Anabel E.-M. Clemen, J. Christof, M. Gebhardt, and Sven Leier for excellent technical help.

The authors' work was supported by the Deutsche Forschungsgemeinschaft (SFB 413, SFB 486, and SPP 1068), and the Friedrich-Baur-Foundation.

REFERENCES

1. Hackney, D. 1994. Evidence for alternating head catalysis by kinesin during microtubule-stimulated ATP hydrolysis. *Proc. Natl. Acad. Sci. USA.* 91:6865–6869.
2. Hancock, W. O., and J. Howard. 1999. Kinesin's processivity results from mechanical and chemical coordination between the ATP hydrolysis cycles of the two motor domains. *Proc. Natl. Acad. Sci. USA.* 96: 13147–13152.
3. Bathe, F., K. Hahlen, R. Dombi, L. Driller, M. Schliwa, and G. Woehlke. 2005. The complex interplay between the neck and hinge domains in kinesin-1 dimerization and motor activity. *Mol. Biol. Cell.* 16:3529–3537.
4. Schafer, F., D. Deluca, U. Majdic, J. Kirchner, M. Schliwa, L. Moroder, and G. Woehlke. 2003. A conserved tyrosine in the neck of a fungal kinesin regulates the catalytic motor core. *EMBO J.* 22:450–458.
5. Kirchner, J., G. Woehlke, and M. Schliwa. 1999. Universal and unique features of kinesin motors: insights from a comparison of fungal and animal conventional kinesins. *Biol. Chem.* 380:915–921.
6. Tripet, B., R. D. Vale, and R. S. Hodges. 1997. Demonstration of coiled-coil interactions within the kinesin neck region using synthetic peptides. Implications for motor activity. *J. Biol. Chem.* 272:8946–8956.
7. Deluca, D., G. Woehlke, and L. Moroder. 2003. Synthesis and conformational characterization of peptides related to the neck domain of a fungal kinesin. *J. Pept. Sci.* 9:203–211.
8. Thormahlen, M., A. Marx, S. Sack, and E. Mandelkow. 1998. The coiled-coil helix in the neck of kinesin. *J. Struct. Biol.* 122:30–41.
9. Mandelkow, E., and K. A. Johnson. 1998. The structural and mechanochemical cycle of kinesin. *Trends Biochem. Sci.* 23:429–433.
10. Schief, W. R., and J. Howard. 2001. Conformational changes during kinesin motility. *Curr. Opin. Cell Biol.* 13:19–28.
11. Romberg, L., D. W. Pierce, and R. D. Vale. 1998. Role of the kinesin neck region in processive microtubule-based motility. *J. Cell Biol.* 140:1407–1416.
12. Su, J. Y., R. S. Hodges, and C. M. Kay. 1994. Effect of chain length on the formation and stability of synthetic α-helical coiled coils. *Biochemistry.* 33:15501–15510.
13. Henningsen, U., and M. Schliwa. 1997. Reversal in the direction of movement of a molecular motor. *Nature.* 389:93–96.
14. Kallipolitou, A., D. Deluca, U. Majdic, S. Lakamper, R. Cross, E. Meyhofer, L. Moroder, M. Schliwa, and G. Woehlke. 2001. Unusual properties of the fungal conventional kinesin neck domain from *Neurospora crassa*. *EMBO J.* 20:6226–6235.
15. Steinberg, G., and M. Schliwa. 1995. The *Neurospora* organelle motor: a distant relative of conventional kinesin with unconventional properties. *Mol. Biol. Cell.* 6:1605–1618.
16. Clemen, A. E., M. Vilfan, J. Jaud, J. Zhang, M. Barmann, and M. Rief. 2005. Force-dependent stepping kinetics of myosin-V. *Biophys. J.* 88:4402–4410.
17. Finer, J. T., R. M. Simmons, and J. A. Spudich. 1994. Single myosin molecule mechanics: piconewton forces and nanometre steps. *Nature.* 368: 113–119.
18. Svoboda, K., and S. M. Block. 1994. Biological applications of optical forces. *Annu. Rev. Biophys. Biomol. Struct.* 23:247–285.
19. Block, S. M., L. S. Goldstein, and B. J. Schnapp. 1990. Bead movement by single kinesin molecules studied with optical tweezers. *Nature.* 348:348–352.
20. Lakamper, S., A. Kallipolitou, G. Woehlke, M. Schliwa, and E. Meyhofer. 2003. Single fungal kinesin motor molecules move processively along microtubules. *Biophys. J.* 84:1833–1843.
21. Asbury, C. L., A. N. Fehr, and S. M. Block. 2003. Kinesin moves by an asymmetric hand-over-hand mechanism. *Science.* 302: 2130–2134.
22. Kozielski, F., S. Sack, A. Marx, M. Thormahlen, E. Schonbrunn, V. Biou, A. Thompson, E. M. Mandelkow, and E. Mandelkow. 1997. The crystal structure of dimeric kinesin and implications for microtubule-dependent motility. *Cell.* 91:985–994.
23. Tomishige, M., and R. D. Vale. 2000. Controlling kinesin by reversible disulfide cross-linking. Identifying the motility-producing conformational change. *J. Cell Biol.* 151:1081–1092.
24. Carter, N. J., and R. A. Cross. 2005. Mechanics of the kinesin step. *Nature.* 435:308–312.
25. Schwaiger, I., C. Sattler, D. R. Hostetter, and M. Rief. 2002. The myosin coiled-coil is a truly elastic protein structure. *Nat. Mater.* 1: 232–235.
26. Thorn, K. S., J. A. Ubersax, and R. D. Vale. 2000. Engineering the processive run length of the kinesin motor. *J. Cell Biol.* 151:1093–1100.
27. Wang, Z., and M. P. Sheetz. 2000. The C-terminus of tubulin increases cytoplasmic dynein and kinesin processivity. *Biophys. J.* 78:1955–1964.
28. Navone, F., J. Niclas, N. Hom-Booher, L. Sparks, H. D. Bernstein, G. McCaffrey, and R. D. Vale. 1992. Cloning and expression of a human kinesin heavy chain gene: interaction of the COOH-terminal domain with cytoplasmic microtubules in transfected CV-1 cells. *J. Cell Biol.* 117:1263–1275.